Global Biogeochemical Cycles

Supporting Information for

Sources of uncertainties in 21st century projections of potential ocean ecosystem stressors

[1]Thomas L. Frölicher, [2]Keith B. Rodgers, [3]Charles Stock, [4]William W. L. Cheung

[1]Environmental Physics, Institute of Biogeochemistry and Pollutant Dynamics, ETH Zürich, Switzerland

[2]Program in Atmospheric and Oceanic Sciences, Princeton University, USA

[3]NOAA Geophysical Fluid Dynamics Laboratory, Princeton University Forrestal Campus, 201 Forrestal Road, Princeton, USA

[4]NF-UBC Nereus Program & Changing Ocean Research Unit, Institute for the Oceans and Fisheries, The University of British Columbia, Vancouver, B. C., Canada.

Contents of this file

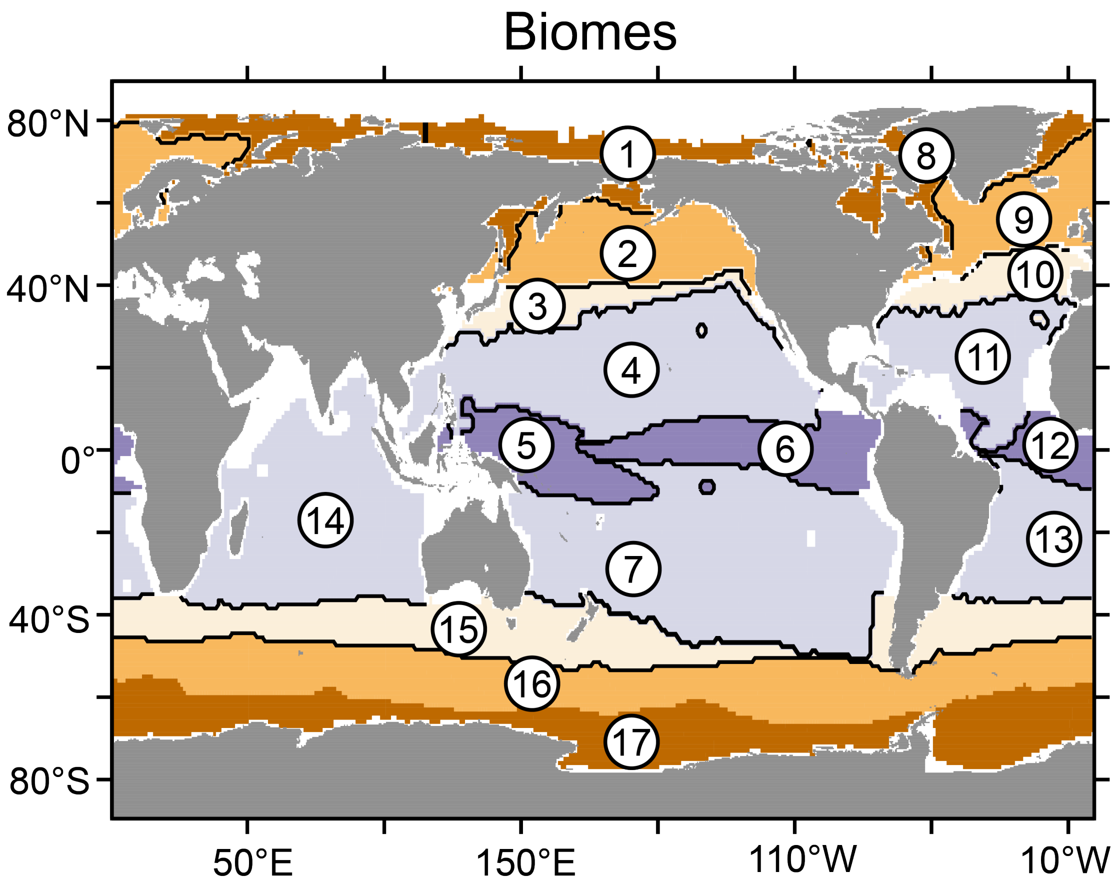

Figure S1: Biogeographical biome map adapted from Fay and McKinley (2014). Ice biomes (ICE) are in brown, subpolar seasonally stratified (SPSS) biomes are in orange, subtropical seasonally stratified biomes (STSS) are in yellow, subtropical permanently stratified biomes (STPS) are in light blue and equatorial biomes (EQ) are in dark blue. 1) NP ICE, 2) NP SPSS, 3) NP STSS, 4) NP STPS, 5) West EQ Pac, 6) East EQ Pac, 7) SP STPS, 8) NA ICE, 9) NA SPSS, 10) NA STSS, 11) NA STPS, 12) EQ Atl, 13) SA STPS, 14) IND STPS, 15) SO STSS, 16) SP SPSS, 17) SO ICE. White areas indicate ocean areas that are excluded from the analysis.

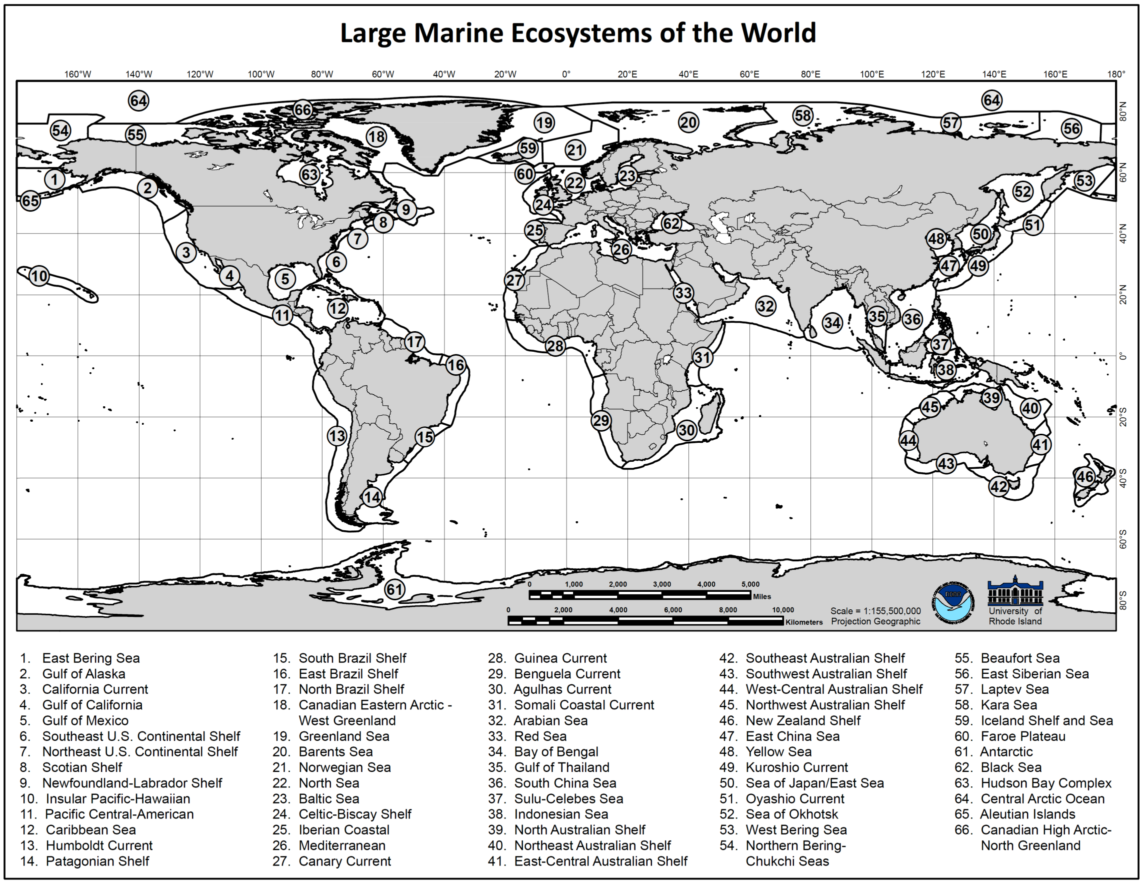

Figure S2. Map showing 66 Large Marine Ecosystems that are used for detailed analysis in this study. Source: www.lme.noaa.gov.

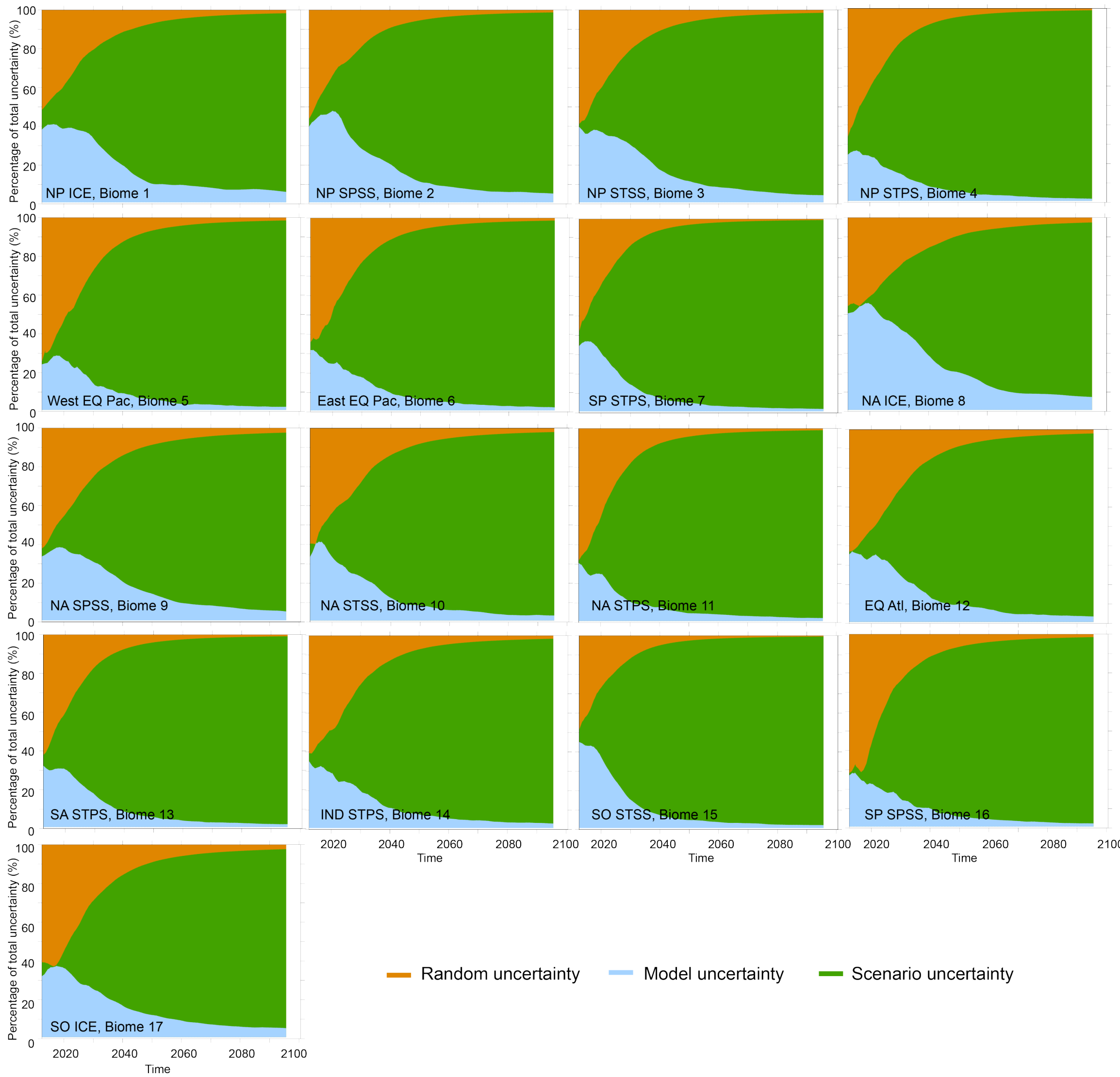

Figure S3. Fraction of total uncertainty in projected annual mean surface pH explained by internal variability (orange), model uncertainty (blue) and scenario uncertainty (green) for 17 biogeographical biomes.

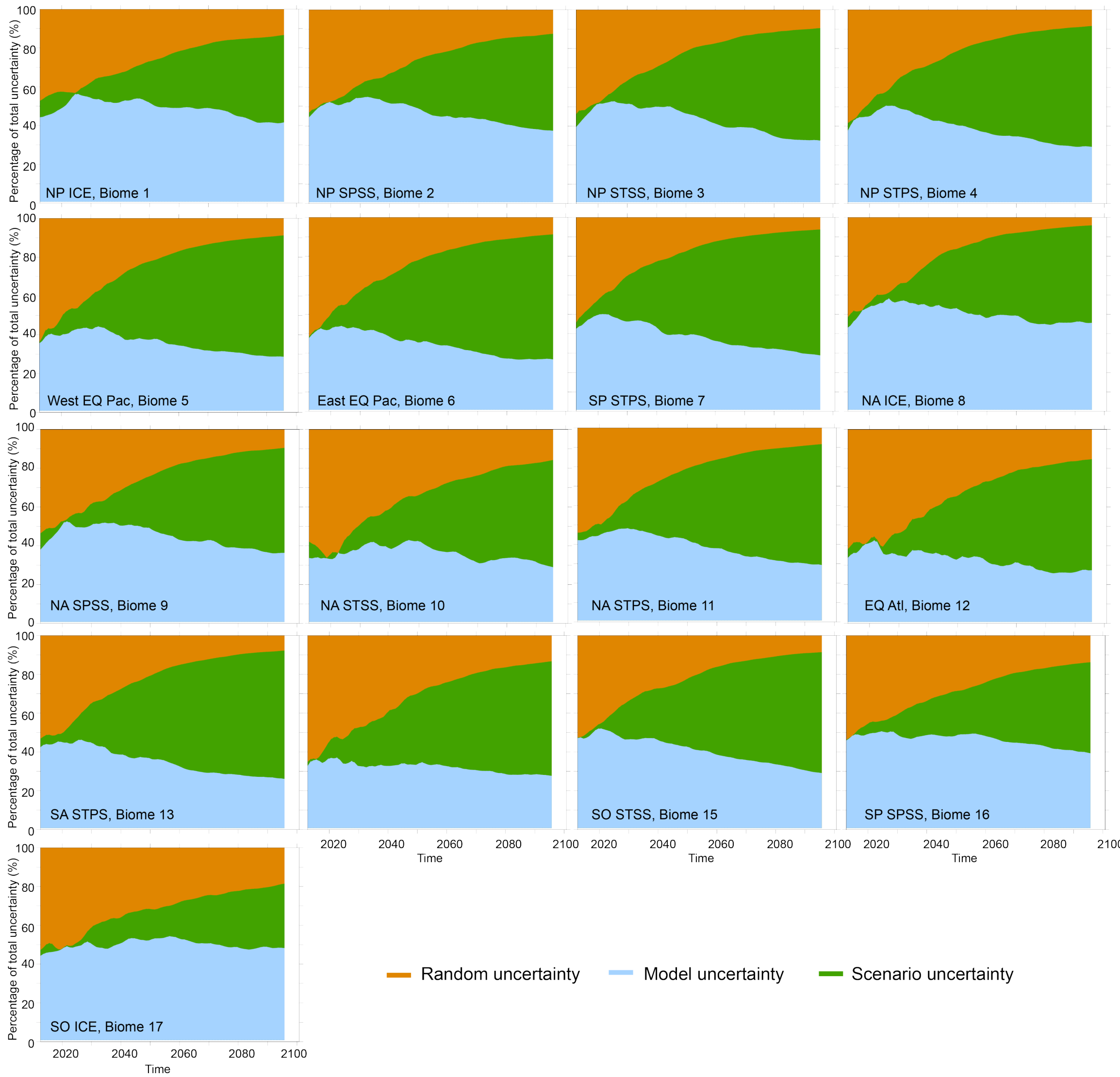

Figure S4. Fraction of total uncertainty in projected annual mean sea surface temperature explained by internal variability (orange), model uncertainty (blue) and scenario uncertainty (green) for 17 biogeographical biomes.

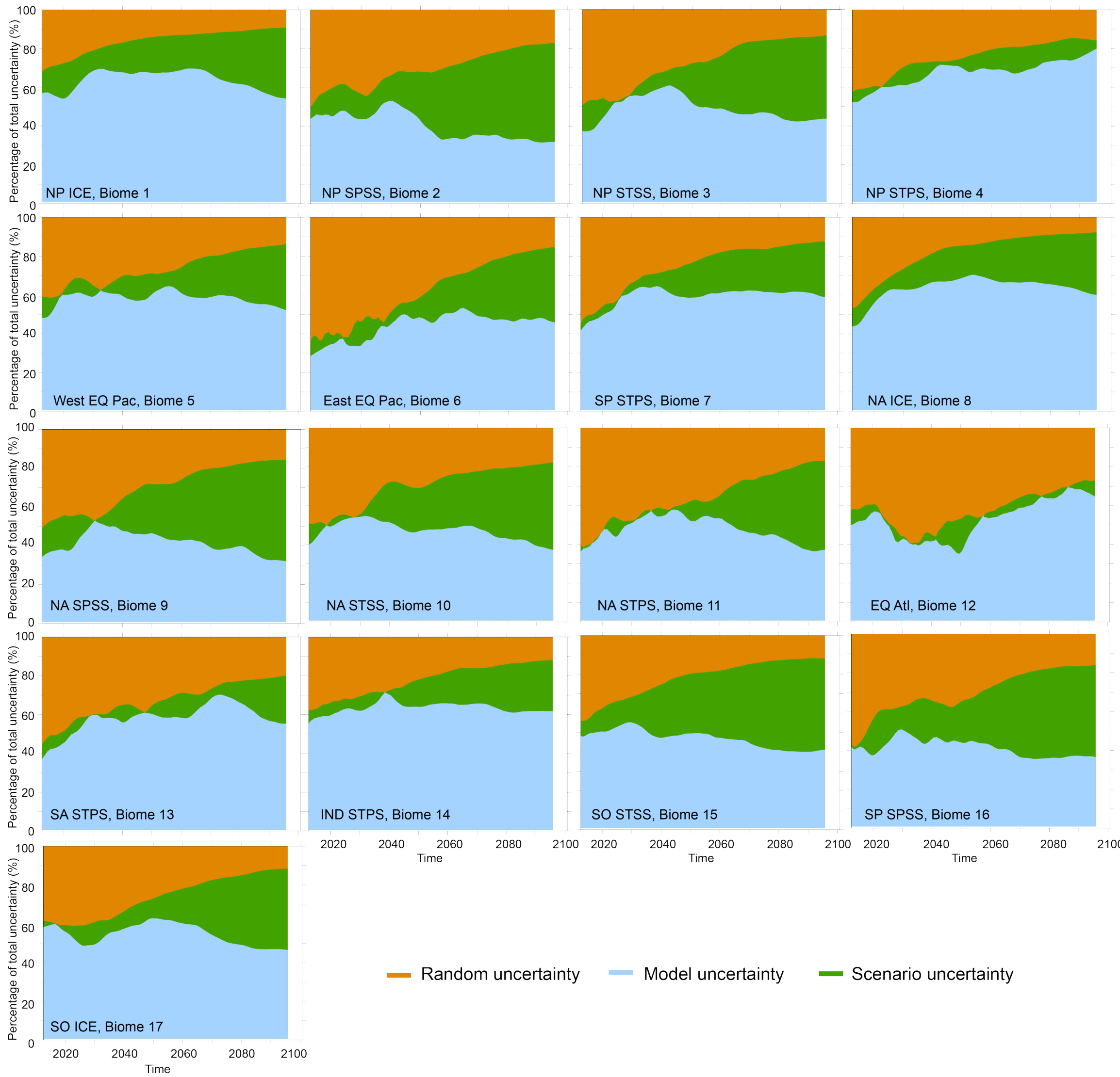

Figure S5. Fraction of total uncertainty in projected annual mean dissolved oxygen concentration averaged over 100-600 meter depth explained by internal variability (orange), model uncertainty (blue) and scenario uncertainty (green) for 17 biogeographical biomes.

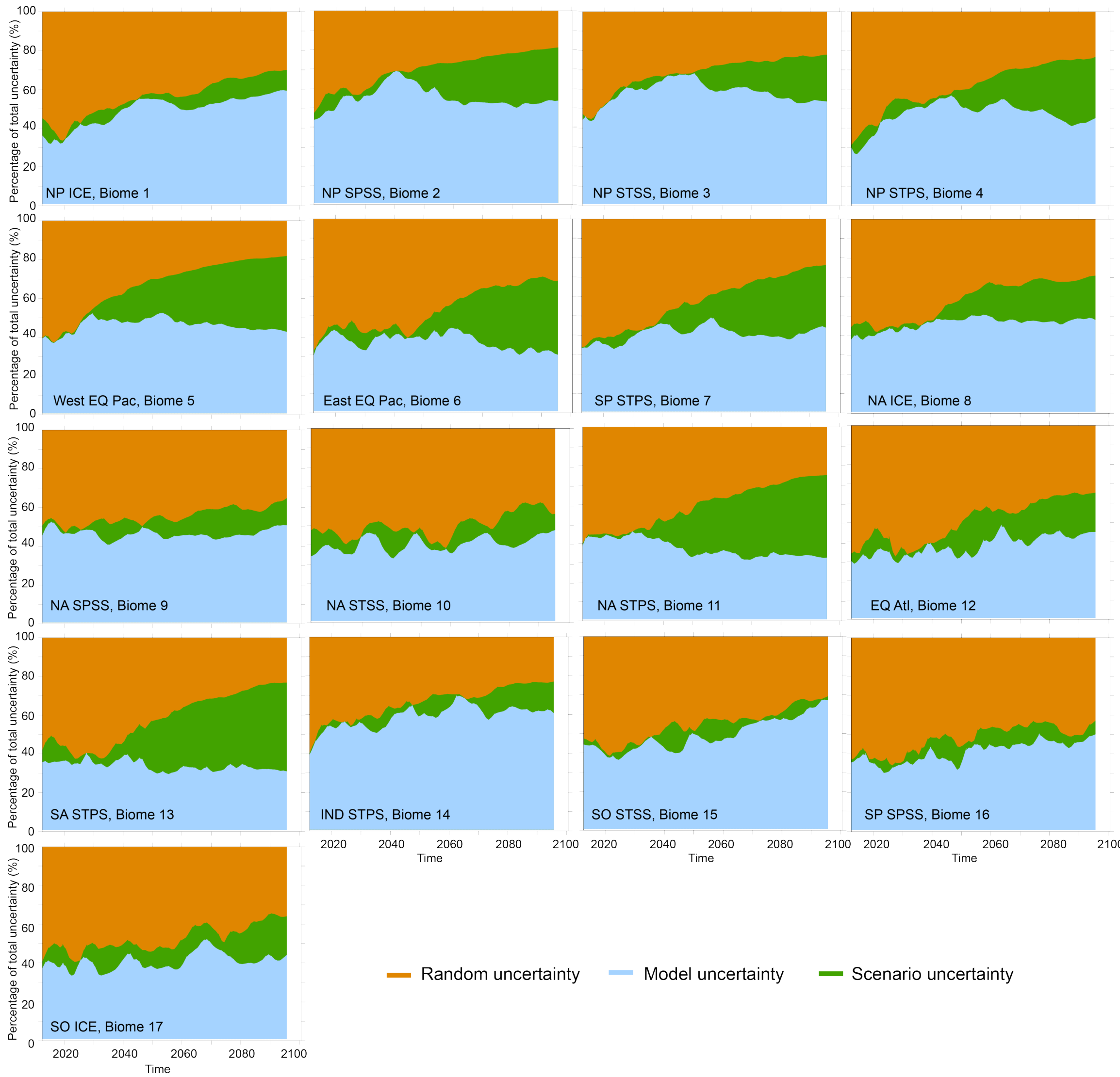

Figure S6. Fraction of total uncertainty in projected annual mean net primary productivity integrated over top 100 meters explained by internal variability (orange), model uncertainty (blue) and scenario uncertainty (green) for 17 biogeographical biomes.

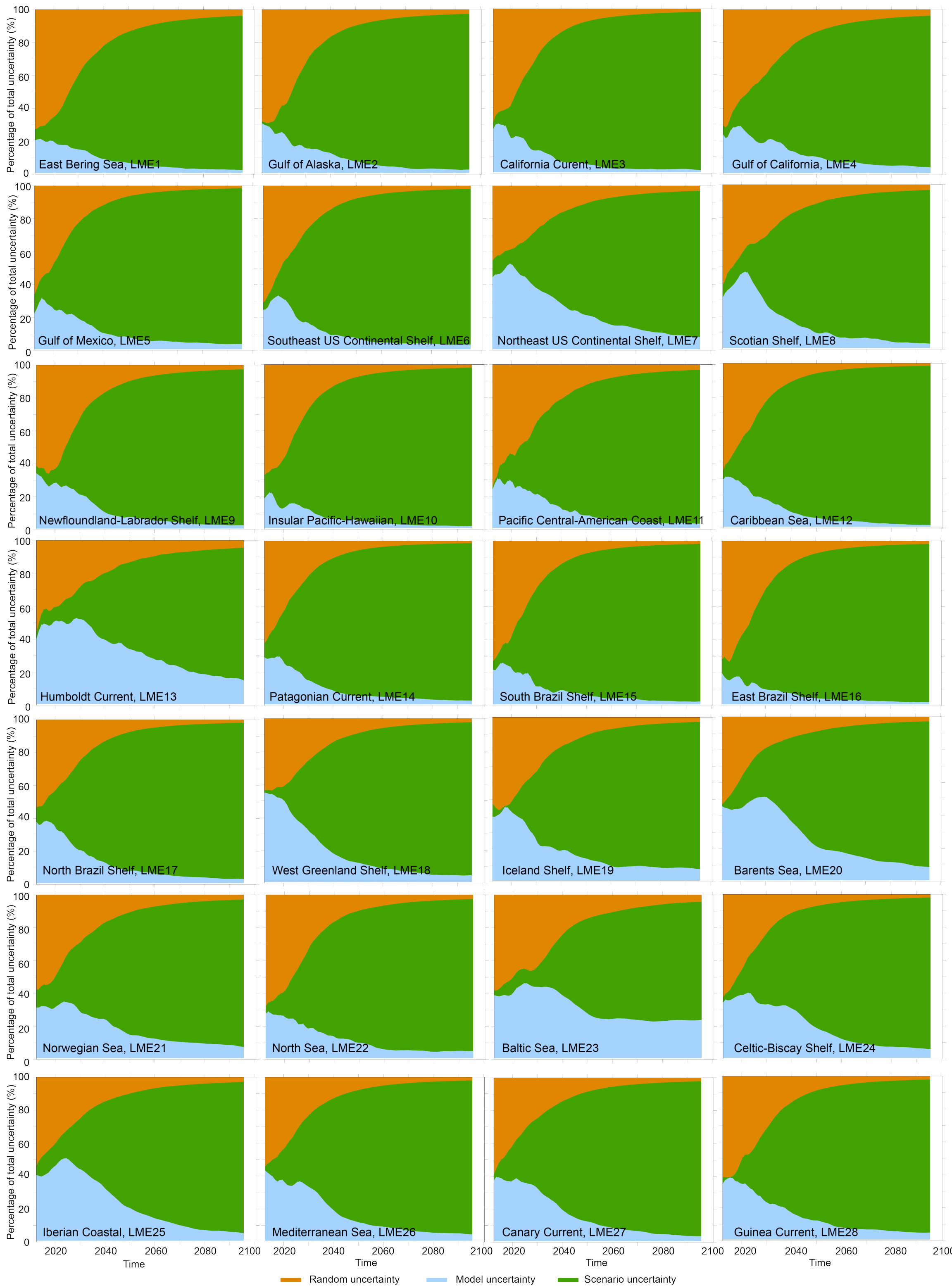

Figure S7. Fraction of total uncertainty in projected annual mean surface pH explained by internal variability (orange), model uncertainty (blue) and scenario uncertainty (green) for large marine ecosystems areas 1-28.

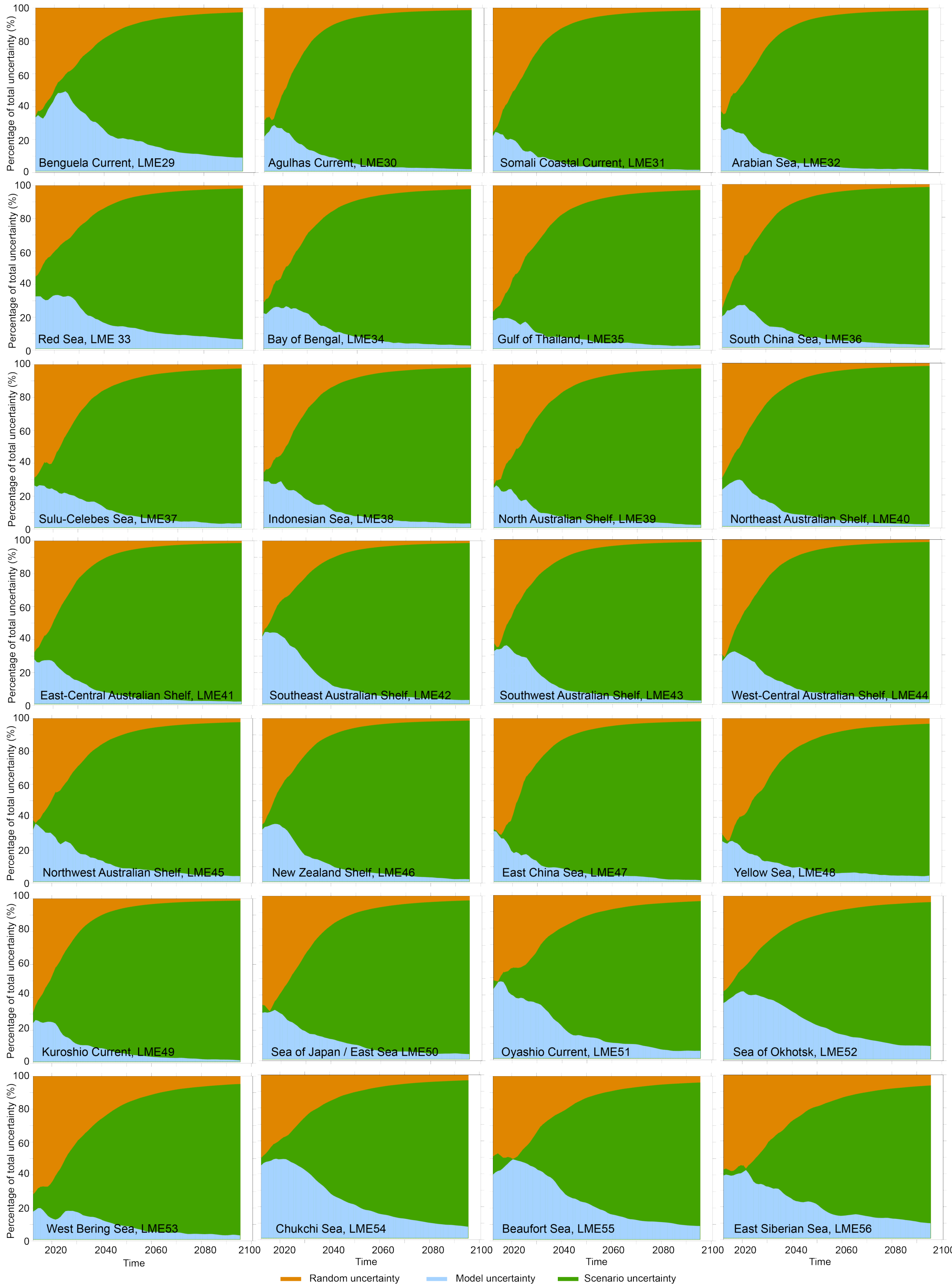

Figure S8. Fraction of total uncertainty in projected annual mean surface pH explained by internal variability (orange), model uncertainty (blue) and scenario uncertainty (green) for large marine ecosystems areas 29-56.

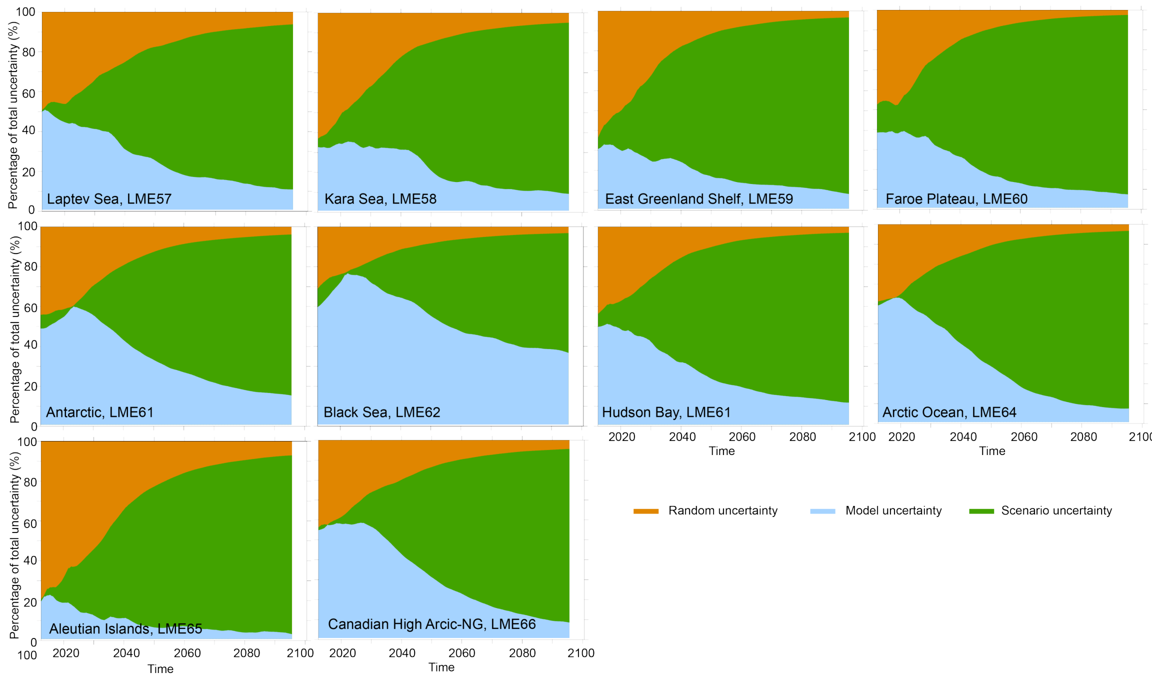

Figure S9: Fraction of total uncertainty in projected annual mean surface pH explained by internal variability (orange), model uncertainty (blue) and scenario uncertainty (green) for large marine ecosystems areas 57-66.

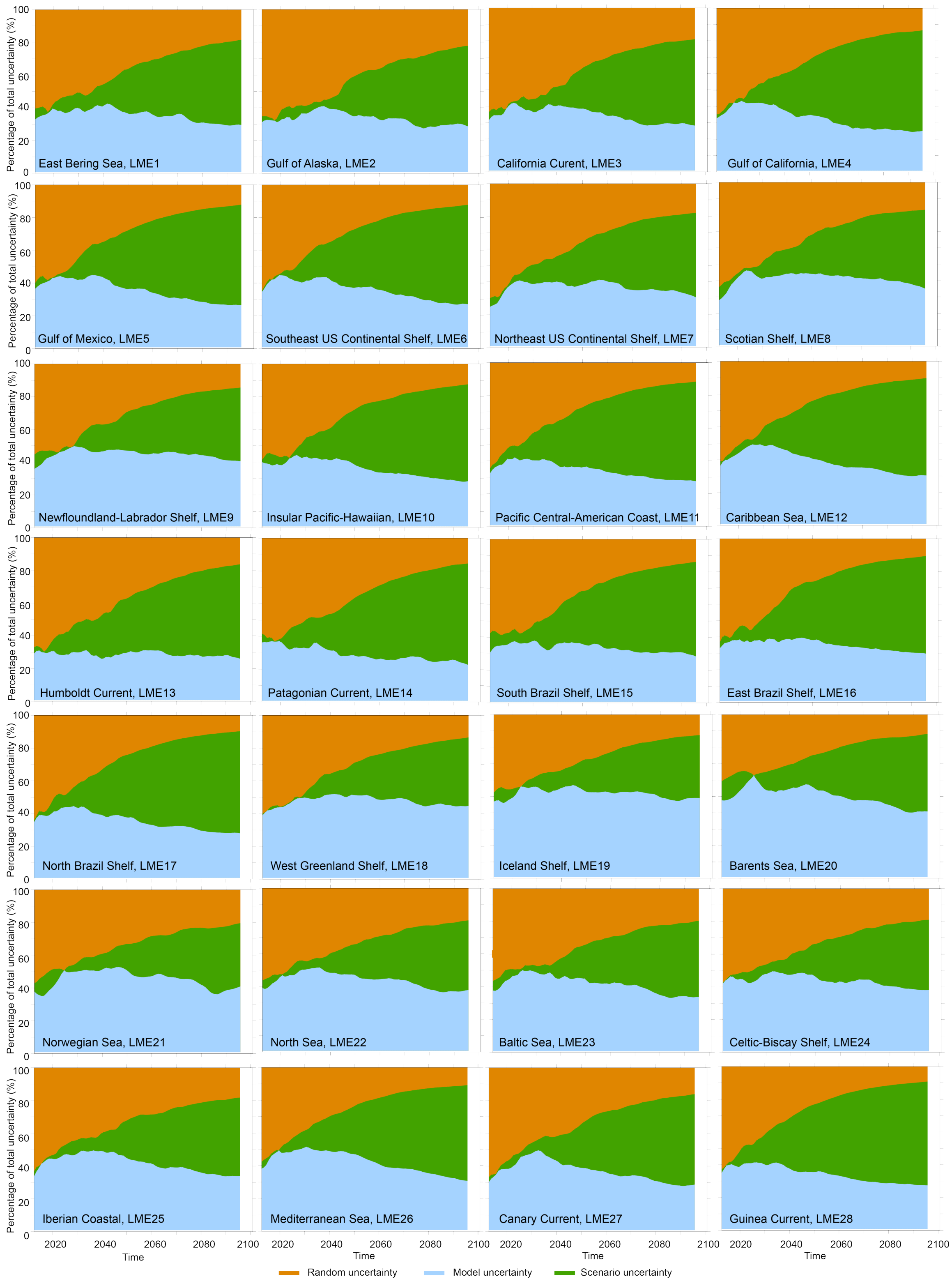

Figure S10. Fraction of total uncertainty in projected annual mean sea surface temperature explained by internal variability (orange), model uncertainty (blue) and scenario uncertainty (green) for large marine ecosystems areas 1-28.

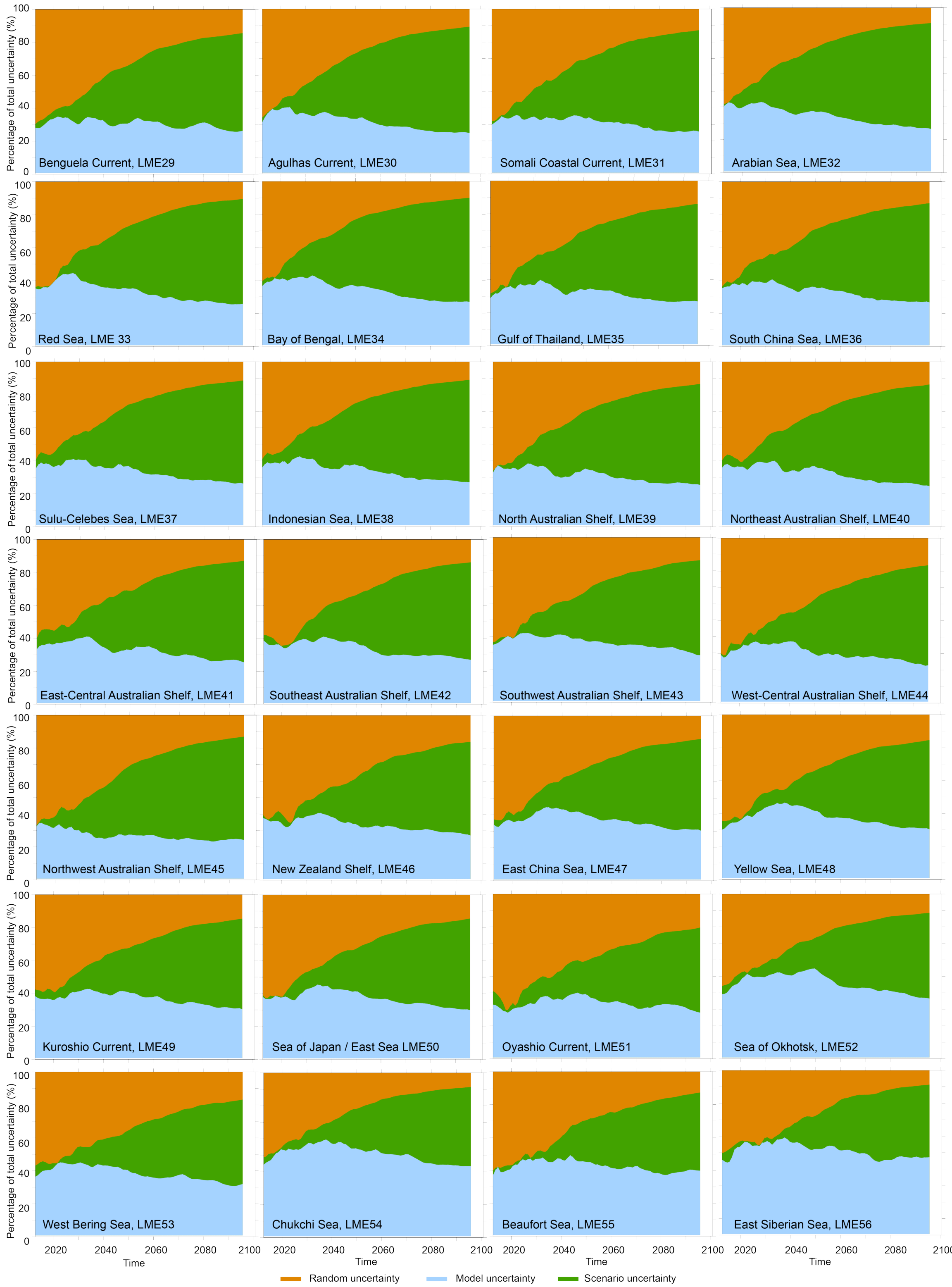

Figure S11. Fraction of total uncertainty in projected annual mean sea surface temperature explained by internal variability (orange), model uncertainty (blue) and scenario uncertainty (green) for large marine ecosystems areas 29-56.

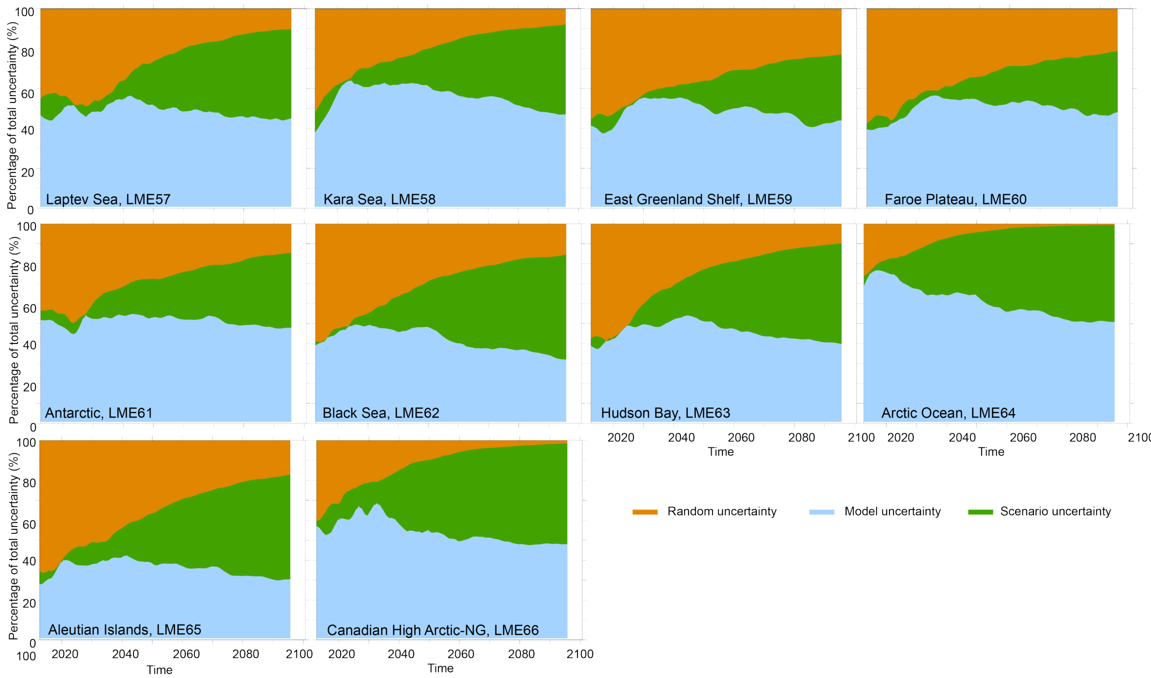

Figure S12. Fraction of total uncertainty in projected annual mean sea surface temperature explained by internal variability (orange), model uncertainty (blue) and scenario uncertainty (green) for large marine ecosystems areas 57-66.

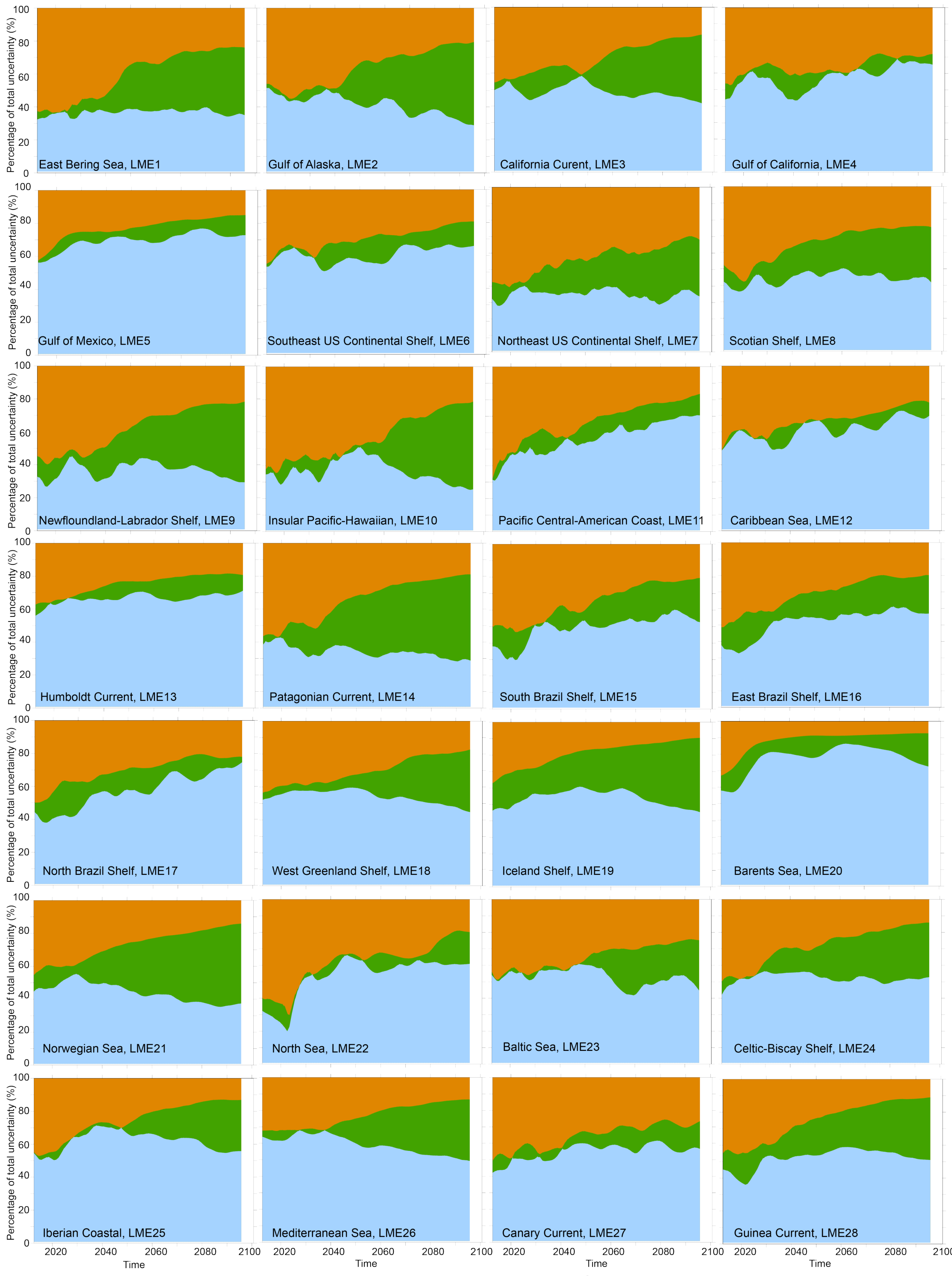

Figure S13. Fraction of total uncertainty in projected annual mean dissolved oxygen averaged over 100-600 meter depth explained by internal variability (orange), model uncertainty (blue) and scenario uncertainty (green) for large marine ecosystems areas 1-28.

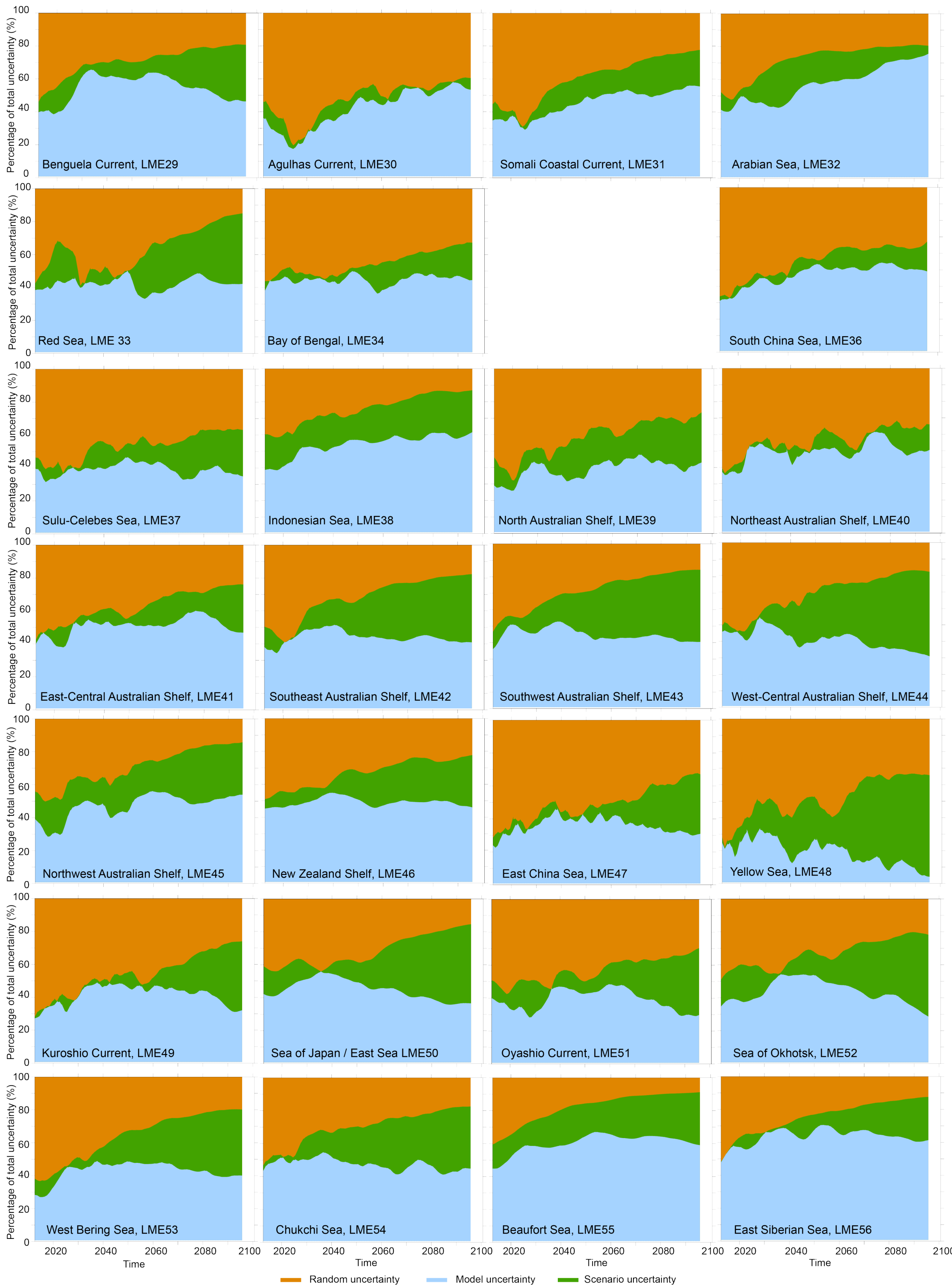

Figure S14. Fraction of total uncertainty in projected annual mean dissolved oxygen averaged over 100-600 meter depth explained by internal variability (orange), model uncertainty (blue) and scenario uncertainty (green) for large marine ecosystems areas 29-56.

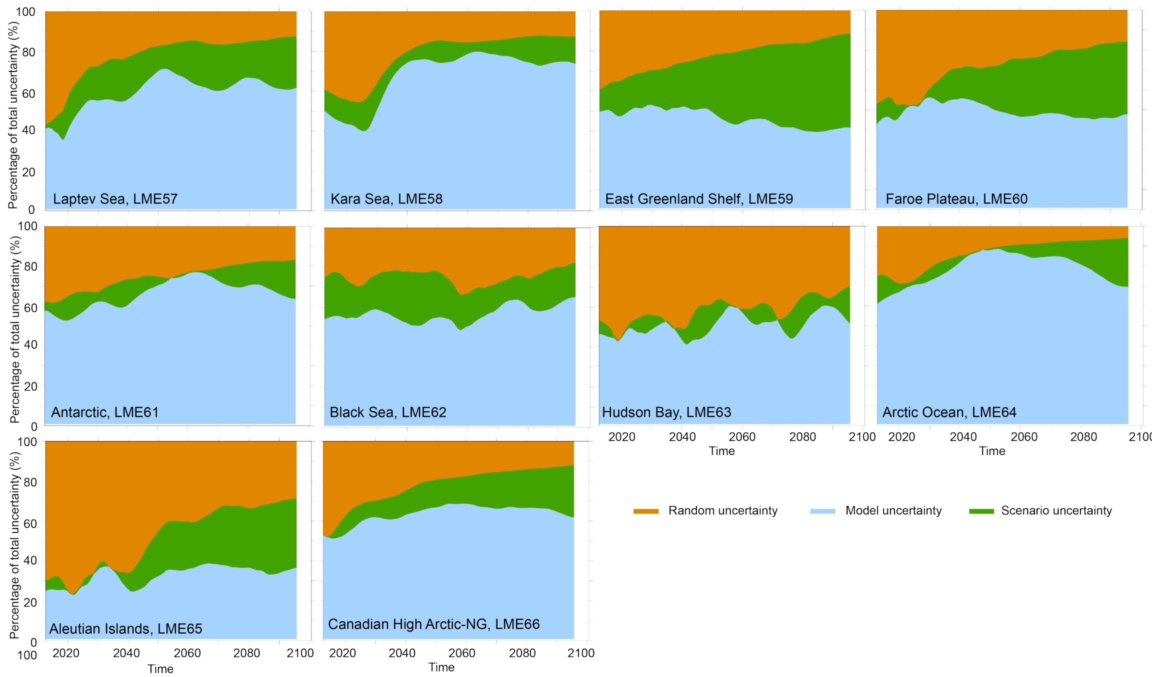

Figure S15. Fraction of total uncertainty in projected annual mean dissolved oxygen averaged over 100-600 meter depth explained by internal variability (orange), model uncertainty (blue) and scenario uncertainty (green) for large marine ecosystems areas 57-66.

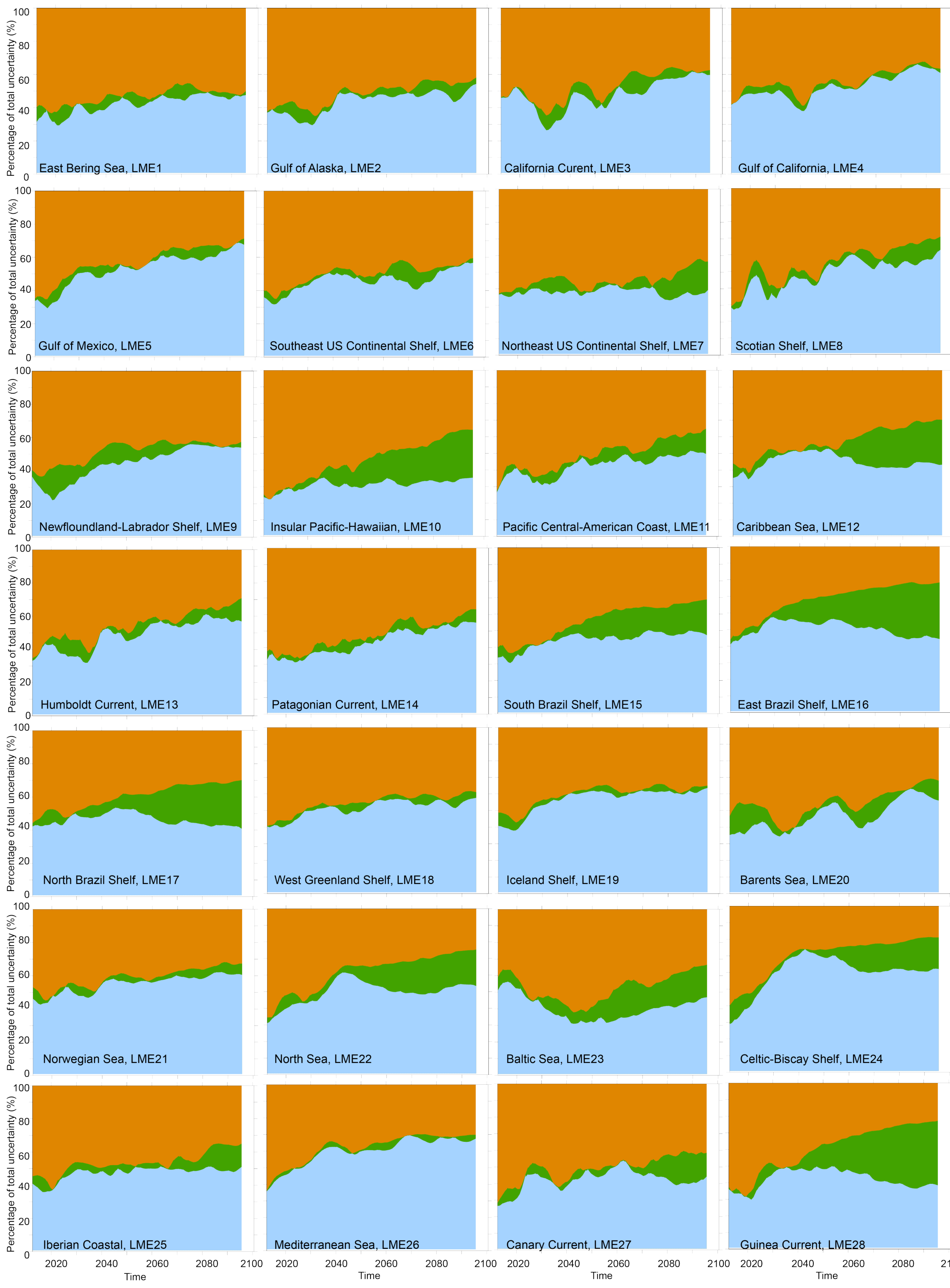

Figure S16. Fraction of total uncertainty in projected annual mean global net primary production integrated over top 100 meters explained by internal variability (orange), model uncertainty (blue) and scenario uncertainty (green) for large marine ecosystems areas 1-28.

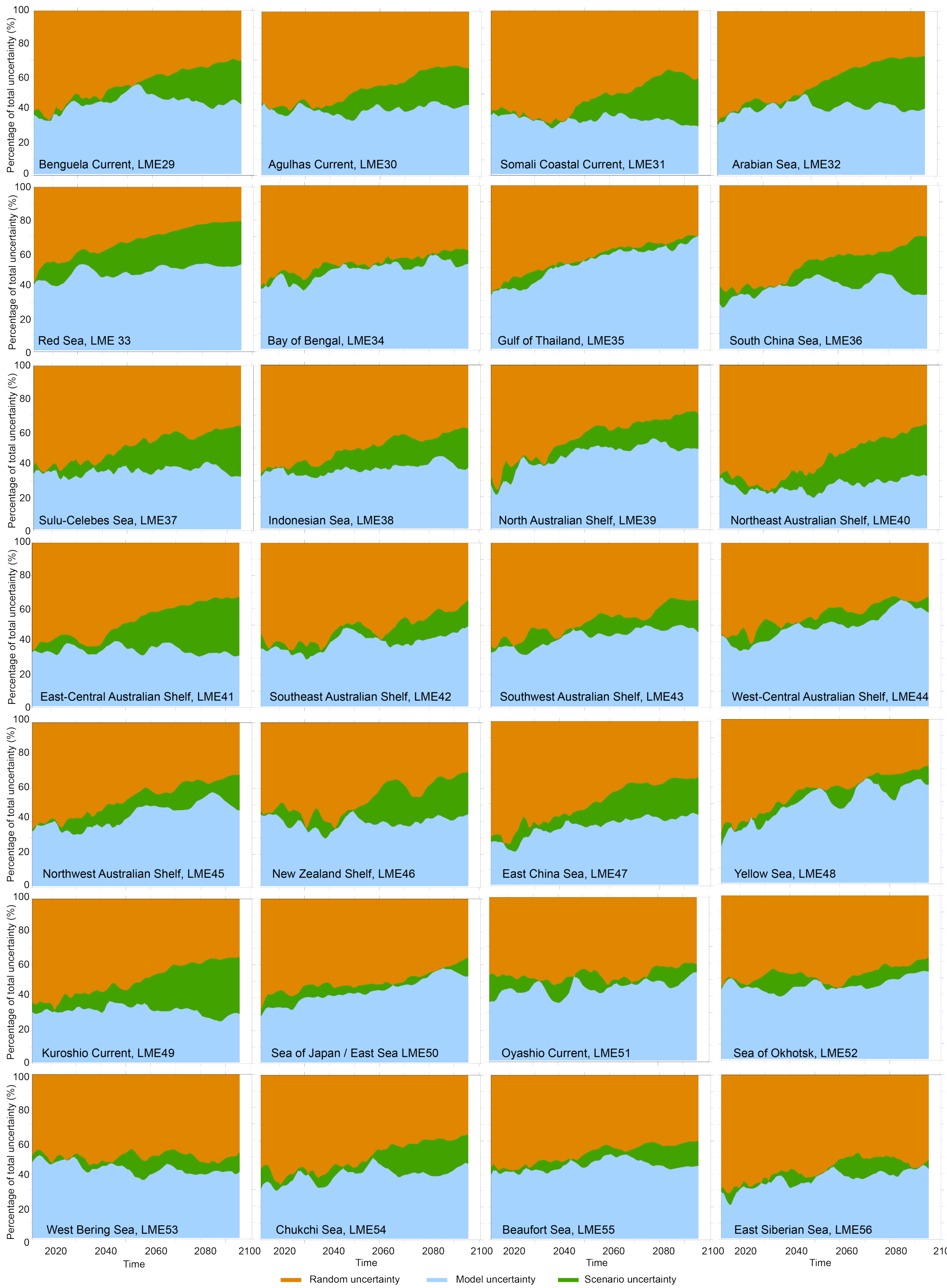

Figure S17. Fraction of total uncertainty in projected annual mean global net primary production integrated over top 100 meters explained by internal variability (orange), model uncertainty (blue) and scenario uncertainty (green) for large marine ecosystems areas 29-56.

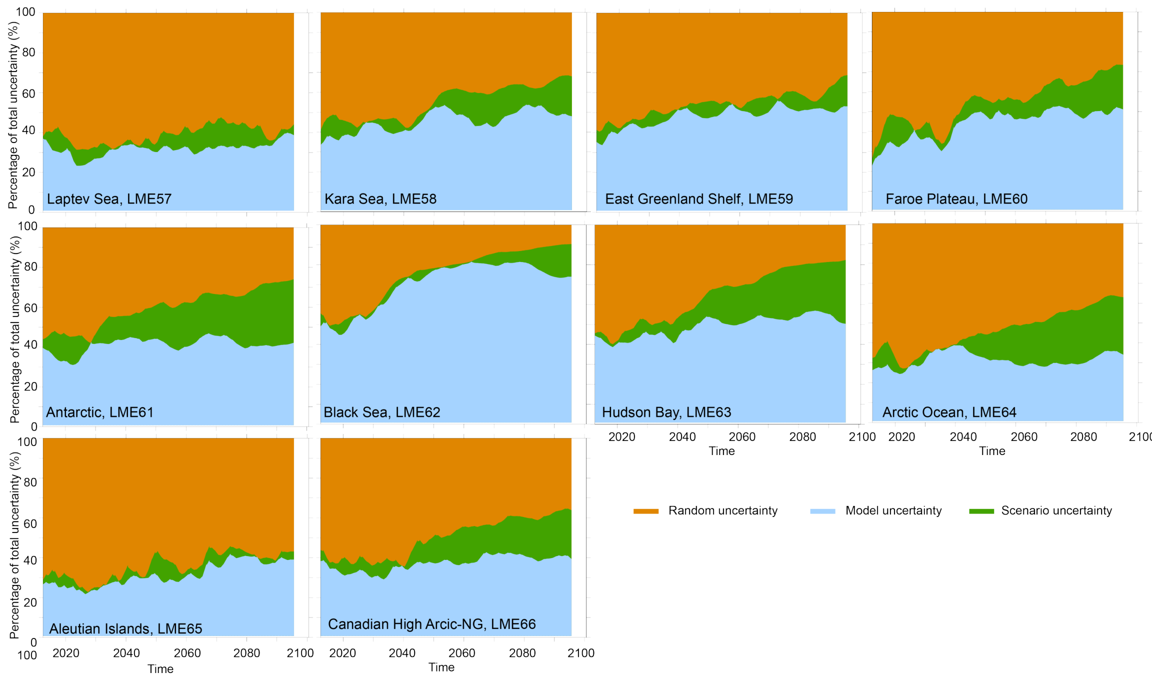

Figure S18. Fraction of total uncertainty in projected annual mean global net primary production integrated over top 100 meters explained by internal variability (orange), model uncertainty (blue) and scenario uncertainty (green) for large marine ecosystems areas 57-66.

Model	Surface pH	SST	O_2 (100-600)	NPP	References
CanSM2	xo996	xo996		xo	Arora et al. [2011]
CNRM-CM5		xo850			Voldoire et al. [2013]
IPSL-CM5A-LR	xo1000	xo1000	xo1000	xo1000	Dufresne et al. [2013]
IPSL-CM5A-MR	xo300	xo300	xo300	xo300	Dufresne et al. [2013]
IPSL-CM5B-LR	x300		x300	x300	Dufresne et al. [2013]
MIROC-ESM		xo680			Watanabe et al. [2011]
MPI-ESM-LR	xo1000		xo1000	xo1000	Giorgetta et al. [2013]
MPI-ESM-MR	xo1000	xo1000	xo1000	xo1000	Giorgetta et al. [2013]
MRI-CGCM3/MRI-ESM1	x			x	Yukimoto et al. [2012]
CCSM4		xo1051			Gent et al. [2011]
NorESM1-ME		xo252	x	xo	Bentsen et al. [2013]
GFDL-CM3		xo800			Griffies et al. [2012]
GFDL-ESM2G	xo500	xo500	xo500	xo500	Dunne et al. [2012]
GFDL-ESM2M	xo500	xo500	xo500	xo500	Dunne et al. [2012]
GISS-E2-H		xo281			Shindell et al. [2013]
GISS-E2-R		xo531			Shindell et al. [2013]
CESM1-CAM5		xo319			Meehl et al. [2012]
BCC_CSM1-1		xo500			Wu et al. [2014]
BCC-CSM1-1-m		x400			Wu et al. [2014]
CESM-BGC				x	Lindsay et al. [2014]
Total	9/7/8	16/15/16	8/6/7	10/8/7	

Table S1. Models and variables used in this study. Black crosses indicate data over the period 1950 to 2100 following the RCP8.5 scenario, black circles indicate data following the RCP2.6 scenario, and numbers indicate the length of the control simulation.

References

Arora, V. K. et al. (2013), Carbon-concentration and carbon-climate feedbacks in CMIP5 Earth System Models. *J. Climate*, **26**, 5289-5314.

Bentsen, M., et al. (2012) The Norwegian earth system model, NorESM1-M – Part 1: Description and basic evaluation, *Geosci. Model Dev. Discuss.*, **5**, 2843-2931.

Dufresne, J.-L., et al. (2013) Climate change projections using the IPSL-CM5 Earth System Model: from CMIP3 to CMIP5, *Clim Dyn*., **40**, 9-10, 2123-2165.

Dunne, J. P. et al. (2012) GFDL's ESM2 global coupled climate-carbon earth system models part I: Physical formulation and baseline simulation characteristics, *J. Climate*, **25**, 6646-6665.

Fay, A. R., G. A. McKinley (2014), Global open-ocean biomes: mean and temporal variability. *Earth Syst. Sci. Data*, **6**, 273-284.

Gent, P. R., et al. (2011), The Community Climate System Model version 4, *J. Climate*, **24**, 4973-4991.

Giorgetta, M. A., et al. (2013), Climate and carbon cycle changes from 1850 to 2100 in MPI-ESM simulations for the coupled model intercomparison project 5, *J. Adv. Model. Earth Syst.* **5**, 572-597.

Griffies, S. M., et al. (2011), The GFDL CM3 Coupled Climate Model Characteristics of the ocean and sea ice simulations, *J. Climate*, **24**, 3520-3544.

Lindsay, K., et al. (2014), Preindustrial control and 20th century carbon cycle experiments with the Earth System Model CESM1(BGC). *J. Climate*, **27**, 8981-9005.

Meehl, G. A., J. M. Arblaster, J. T. Fasullo, A. Hu, K. E. Trenberth (2011), Model-based evidence of deep-ocean heat uptake during surface-temperature hiatus periods, *Nature Clim. Change*, **1**, 360-364.

Shindell, D. T., et al. (2013), Interactive ozone and methane chemistry in GISS-E2 historical and future climate simulations. *Atmos. Chem. Phys.*, **13**, 2653-2689.

Voldoire, A. et al. (2013), The CNRM-CM5.1 global climate model: description and basic evaluation, *Clim. Dyn*. **40**, 2091-2121.

Watanabe, et al. (2011), MIROC-ESM: coupled description and basic results of CMIP5-20c3m experiments. *Geosci. Model Dev.*, **4**, 845-872.

Wu, T., et al. (2014), An overview of BCC climate system model development and application for climate change studies, *J. Meteor. Res*., **28**, 34-56.

Yukimoto, S., et al. (2012), A new global climate model of Meteorological Research Institute: MRI-CGCM3 – model description and basic performance, *J. Meteor. Soc. Japan*, **90A**, 23-64.